Available online at www.sciencedirect.com

ScienceDirect

www.elsevier.com/locate/jes

JES JOURNAL OF ENVIRONMENTAL SCIENCES

www.jesc.ac.cn

In-situ observations of internal dissolved heavy metal release in relation to sediment suspension in lake Taihu, China

Tingfeng Wu[1,*], *Guangwei Zhu*[1], *Jianghai Chen*[2], *Tengteng Yang*[3]

[1] *State Key Laboratory of Lake Science and Environment, Nanjing Institute of Geography and Limnology, Chinese Academy of Sciences, Nanjing 210008, China*

[2] *Shanghai Investigation Design & Research Institute Co., Ltd., Shanghai 200434, China*

[3] *University of Chinese Academy of Sciences, Beijing 100049, China*

ARTICLE INFO

Article history:
Received 17 February 2020
Revised 2 May 2020
Accepted 3 May 2020
Available online 7 June 2020

Keywords:
Heavy metals
Sediment suspension
Process observation
Eutrophication

ABSTRACT

Despite laboratory experiments that have been performed to study internal heavy metal release, our understanding of how heavy metals release in shallow eutrophic lakes remains limited for lacking *in-situ* evidence. This study used automatic environmental sensors and a water sampling system to conduct high-frequency *in-situ* observations (1-hr intervals) of water environmental variables and to collect water samples (3-hr intervals), with which to examine the release of internal heavy metals in Lake Taihu, China. Under conditions of disturbance by strong northerly winds, sediment resuspension in both the estuary area and the lake center caused particulate heavy metal resuspension. However, the patterns of concentrations of dissolved heavy metals in these two areas were complex. The concentrations of dissolved Se and Mo increased in both areas, indicating that release of internal dissolved Se and Mo is triggered by sediment resuspension. The concentrations of dissolved Ni, Zn, As, Mn, Cu, V, and Co tended to increase in the estuary area but decrease in the lake center. The different trends between these two areas were controlled by pH and cyanobacteria, which are related to eutrophication. During the strong northerly winds, the decrease in concentrations of dissolved heavy metals in the lake center was attributable primarily to absorption by the increased suspended solids, and to growth-related assimilation or surface adsorption by the increased cyanobacteria. The findings of this study suggest that, short-term changes of environmental conditions are very important in relation to reliable monitoring and risk assessment of heavy metals in shallow eutrophic lakes.

Introduction

Enriched heavy metals in lake sediments can be released back to the overlying water under changing environmental conditions, which could pose serious threat to lake ecosystems and human health owing to their long-term persistence, toxicity, and bioaccumulation potential (Eggleton and Thomas, 2004; Jonge et al., 2012; Li et al., 2018; Wang et al., 2020). In shallow lakes, sediments can become resuspended by strong hydrodynamic disturbances (Hofmann et al., 2008; Jin and Ji, 2001; Tang et al., 2020), and pollutants within the sediments can be transmitted directly to the overlying water, causing secondary pollution (Beutel et al., 2008; Eggleton and Thomas, 2004; Geng et al., 2015 Guo et al., 2018). Previous stud-

* Corresponding author.
E-mail: tfwu@niglas.ac.cn (T. Wu).

https://doi.org/10.1016/j.jes.2020.05.004
1001-0742/

ies have suggested that heavy metal content in suspended solids (SS) might be substantially higher than in the bed sediments (Dong et al., 2019; Zhu et al., 2005a). Despite the importance of internal heavy metal release, only a few studies have examined (with high temporal resolution) the *in-situ* processes that drive the release of internal heavy metals from sediments in shallow lakes.

In addition to sampling location, depth, and density (Hou et al., 2017; Jiang et al., 2012), sampling frequency might be important in relation to the risk assessment of heavy metal pollution in shallow lakes. Based on *in-situ* observations, it has been established that sediments of shallow lakes are frequently disturbed by wind-induced hydrodynamics, and that the concentrations of SS in the overlying water generally follows a short-term unimodal or multimodal pattern during such disturbance (Cózar et al., 2005; Tang et al., 2020; Wu et al., 2019). It suggests that heavy metal release from sediments might exhibit similar characteristics. However, it cannot be guaranteed that the peak concentrations of heavy metals in shallow lakes can be captured using low-frequency sampling, which means the reliability of any assessment of heavy metal pollution from sediments might be compromised.

Moreover, the water environmental variables (e.g., pH, dissolved oxygen, redox potential, and chlorophyll *a* (Chl*a*)) are continually varying in shallow eutrophic lakes (Ding et al., 2012; Paerl and Paul, 2012; Pokrovsky and Shirokova, 2013). These variations of the environmental variables can result in rapid changes of the concentrations of dissolved heavy metals within the water column, as proven by numerous laboratory experiments (Jonge et al., 2012; Linge and Oldham, 2002; Liu et al., 2017). For example, based on laboratory experiments, Linge and Oldham (2002) found water pH varied quickly during hydrodynamic disturbances, which led to corresponding release of dissolved As from the sediments. However, sometimes, laboratory results cannot truly reflect the release process that occurs in natural waterbodies. *In-situ* observations are required to supply direct evidence of internal heavy metal release in shallow eutrophic lakes. Fortunately, recent technological advances have led to the development of high-frequency wireless hydrometeorological sensors (Porter et al., 2005; Wu et al., 2019) and automatic water sampling systems suitable for use in conducting *in-situ* observation of the release processes of internal heavy metals in shallow lakes through high-frequency monitoring.

In this study, we conducted *in-situ* high-frequency observations of the release processes of heavy metals from sediments in a large shallow eutrophic lake that experiences severe cyanobacterial blooms. We determined the contents of heavy metal in the sediments, and we used high-frequency observations to examine the patterns in their release when the sediments were resuspended during a strong wind event. The objectives of this study were as follows: (1) to examine the characteristics of internal heavy metals release from sediments in the shallow lake, (2) to compare the release patterns of different types of dissolved heavy metals, and (3) to determine how lake eutrophication might influence the release of dissolved heavy metals.

1. Materials and methods

1.1. Overview of the study area

Lake Taihu is on the southern edge of the Yangtze River Delta, which is one of the most economically developed and densely populated areas of China. Lake Taihu is the third largest freshwater lake in China (Fig. 1) with a surface area of 2338.1 km^2. It is a shallow lake, which has a multiyear average water level of 3 m and an average water depth of only 1.9 m (Qin et al., 2007). The Lake Taihu Basin has a subtropical monsoon climate; annual average temperature ranges from 16.0 to 18.0 °C, and annual average precipitation ranges from 1100 to 1150 mm. The terrain of the basin is high in the west and low in the east. The principal inflows to the lake are mostly on the western side, while the outflows are located on the eastern side. The Tiaoxi River is one of the inflowing rivers that contribute to the water balance of Lake Taihu with a flood season (spring and summer) and a dry season (autumn and winter) (Qin et al., 2007). The inflowing rivers transport various pollutants from the basin directly into western parts of the lake, especially in the flood season. Consequently, these areas receive the majority of the sewage discharges, which causes them to suffer frequent cyanobacterial blooms (Niu et al., 2015).

1.2. In-situ *observation of internal heavy metal release*

Winter is dry and thus represents the optimal season in which to investigate the influence of hydrodynamic disturbances on internal pollutant release in Lake Taihu, primarily because the impact of biological activities on internal pollutant release processes are minimized when the temperature is low (Zhu et al., 2005b). Therefore, the *in-situ* observations were conducted in Lake Taihu during a strong wind event that occurred between 09:00 local time (LT) on December 26, 2018 and 12:00 LT on December 29, 2018. For comparison purposes, two *in-situ* observation stations were established 12.1 km apart in areas plagued by sludge (Shen et al., 2011; Wu et al., 2019): one in the estuary area of the Tiaoxi River (TH1) and the other nearer the center of the lake (TH2) (Fig. 1). To ensure the safety of the instruments and for provision of a stable continuous power supply, the monitoring equipment was installed on a large observation platform at each station.

Each station was equipped with a multiparameter sonde (YSI 6600 V2 Sonde; YSI Inc., USA), which automatically recorded water temperature (±0.01 °C), pH (pH, ±0.01), dissolved oxygen (DO, ±0.01 mg/L), and water depth (±0.001 m) at 1 m above the water sediment interface at hourly intervals. In addition, water samples were collected at 1 m above the water–sediment interface at each station using a remote-controlled automatic water sampling system (FC-9624; Beijing Grasp Technology Co., Ltd., China). Based on weather forecast information, both water sampling systems at the two stations were triggered synchronously via a mobile APP, which prompted collection of 24 water samples at 3-hr intervals at each station. The water samples were held temporarily in a sample storage chamber filled with liquid nitrogen in the sampler. A portable weather station (WX520; Vaisala Inc., Finland) was installed at TH2 to record automatically the air temperature, wind speed, and wind direction at 10 m above the water surface at 1-hr intervals.

On completion of the *in-situ* observations, the equipment and water samples were taken to the laboratory. The data recorded by the sondes and the meteorological equipment (WX520 recorders) were downloaded to a local disk using client software. All water samples were analyzed to determine the dissolved organic carbon (DOC) concentration, loss on ignition that characterizes the content of particulate organic matter in water (LOI-W), Chl*a*, SS, and the concentrations of nine selected dissolved heavy metals: Ni, Zn, As, Mn, Cu, V, Co, Mo, and Se.

1.3. Sediment investigation

Three replicate sediment samples were collected from the bottom sediment at both TH1 and TH2 using a Peterson grab on the day before the *in-situ* observations commenced; these

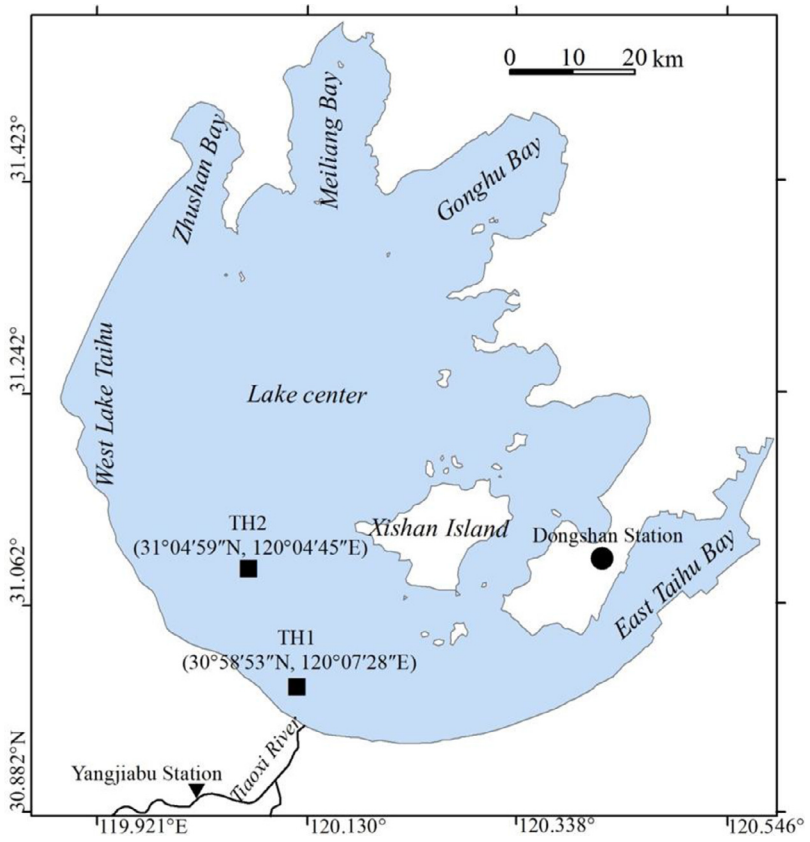

Fig. 1 – Locations of the *in-situ* high-frequency observation stations (TH1 and TH2), Dongshan Station (precipitation and evaporation) and Yangjiabu Station (runoff rate of Tiaoxi River) in Lake Taihu, China.

were subsequently analyzed for their physical and chemical characteristics. After plant residue, shells, and gravel were removed, each sediment sample was divided into two portions using a wooden spatula. One portion was sealed in a polyethylene plastic bag and used for measuring the median grain size and the contents of nine heavy metals. The second portion was placed in an aluminum box with a lid (diameter: 2 cm, height: 1.5 cm) and used for determination of the dry bulk density, water content, and loss on ignition which can characterize the particulate organic matter content of air-dried sediment (LOI-S).

Moreover, considering the influence of the Tiaoxi River, hourly precipitation and evaporation data recorded at the Dongshan Station (Fig. 1) were provided by the National Meteorological Information Center, China, and daily mean runoff rates of the Tiaoxi River to Lake Taihu were collected from Yangjiabu Station (Fig. 1), built by the Ministry of Water Resources, China.

1.4. *Analysis of sediments and water samples*

1.4.1. *Physical and chemical parameters of the sediment samples*

Dry bulk density and water content (Graca et al., 2004): The mass of fresh sediment from the aluminum box and the mass of dry sediment after air-drying were determined using a balance. The ratio of dry sediment mass to the volume of the aluminum box represents the dry bulk density, while the ratio of the difference between the mass of air-dried and fresh sediments to the mass of fresh sediments represents the water content.

Median grain size (Ramaswamy and Rao, 2006): A small amount of air-dried sediment was pretreated by adding a dispersant and then vibrated ultrasonically to remove organic matter and carbonate. The sediment grain size was then determined using a laser particle size analyzer (MasterSizer 2000, Malvern Instruments Ltd., UK).

LOI-S content (Boyle, 2004): The sediment was dried in a crucible at 105 °C and then weighed. The dry sediment was then calcinated at 550 °C for 4 hr before being weighed. The difference in the mass of sediment before and after calcination was then used to calculate the LOI-S content.

1.4.2. *Concentrations of DOC, LOI-W, Chla, and SS of water samples*

The water samples were filtered through a Whatman® GF/F filter with porosity of 0.7 (Fisher Scientific, Fair Lawn, NJ, USA). The DOC concentrations of the filtrates were then determined using a TOC analyzer (Multi N/C 2100, Jena, Germany). After extraction from the membrane filter using ethanol (90%) at 80 °C, the Chl*a* concentrations were determined by spectrophotometry with a phaeopigment correction (Chen and Gao, 2000). Before and after filtration, the membrane filter was dried at 105 °C and weighed. The mass difference of the membrane filter before and after filtration was then divided by the volume of the water sample to calculate the SS concentration. The LOI-W content on the membrane filter after filtration, which was used to calculate the LOI-W concentration,

was determined using a method similar to that used for LOI-S.

1.4.3. *Heavy metal content of sediment and dissolved heavy metal concentrations*

Heavy metal content of sediment: air-dried sediment was digested by adding concentrated nitric acid and hydrogen peroxide repeatedly at an elevated temperature (APHA, 1998; Yin et al., 2014). The heavy metal concentrations, which were used to calculate the heavy metal content of the sediment, were then determined using inductively coupled plasma mass–spectrometry (ICP-MS, Agilent 7700 ×). Dissolved heavy metal concentrations: The water samples were filtered through a Whatman® GF/F filter with porosity of 0.7. The dissolved heavy metal concentrations were then determined using ICP-MS.

To ensure analytical quality, reagent blanks were conducted in parallel with all sample analyses. In all cases, the value of the tested blanks was lower than 5% of the sample values. The USA SPEX^{TM} CLARITAS PPT® mixed multi-element standard solution (CL-CAL-2) was used for instrument calibration. During analysis of the heavy metal content of the sediment, the "National Certified Reference Material-lacustrine sediment" (GBW07309) was used to control the quality of the concentrations in the heavy metal analysis. Recoveries between the measured values and certified values of GBW07309 were in the range 96.3%–110.7%. The relative standard deviation (RSD) of replicates for all elements was within 14.8%. During analysis of the dissolved heavy metal concentrations, the standard solution of rhenium with known concentration, replicates, and blank samples were used to control the quality of the concentrations in the heavy metal analysis. Recoveries between the measured values and known values of the standard solutions of rhenium were in the range 87.5%–106.6%. The RSD of replicates for all elements was lower than 10.0%.

1.5. *Statistical analysis of data*

The Mann–Kendall trend test (M-K test) was applied to analyze the trends of the measured time series:

$$MK = \frac{(A-1)\sqrt{18}}{\sqrt{n(n-1)(2n+5)}} \qquad A = \sum_{i=2}^{n}\sum_{j=1}^{i-1} sign\left(a_i - a_j\right) > 0 \tag{1}$$

$$MK = 0 \qquad A = 0 \tag{2}$$

$$MK = \frac{(A+1)\sqrt{18}}{\sqrt{n(n-1)(2n+5)}} \qquad A < 0 \tag{3}$$

where a positive value of MK indicates an increasing trend in the measured time series, and vice versa. |MK| values greater than 1.64 and 2.32 were significant at the 95% ($P < 0.05$) and 99% ($P < 0.01$) levels, respectively (Wu et al., 2018). The program for the trend test of the measured series was written in Fortran using the Intel® Visual Fortran Compiler (Intel® Inc., USA).

A map of Lake Taihu was generated using ArcGIS 10.2 (Esri Inc., USA). The concentrations of the water quality parameters were expressed as the mean ± standard deviation (SD). An independent-sample T Test was used to compare the means, and differences were reported by statistical significance (P). A bivariate correlation was used to calculate the Pearson's correlation coefficient (r) and significance level. The T Test and bivariate correlations were processed using SPSS® 18.0 software (SPSS® Inc., Chicago, IL, USA).

2. Results

2.1. *Physical and chemical characteristics of sediments*

The physical and chemical characteristics of sediments at TH1 and TH2 are shown in Table 1. The median grain size, dry bulk density, water content, or LOI-S of sediments between these two stations had no significant difference.

Sediment Mn content was the highest and sediment Se content was the lowest (Table 2). The contents of sediment Ni, Zn, As, and Mn were 1.2–2.1 times greater than the corresponding background values, and the differences were greatest for Ni and Zn. The contents of sediment Zn, Mo, and Se were significantly different between the two stations and all were higher at TH1. The contents of the other heavy metals in the sediments at TH1 and TH2 were not significantly different.

2.2. *Hydrometeorological factors*

During the period of *in-situ* observation (from 09:00 LT on December 26 to 12:00 LT on December 29, 2018), total precipitation was 7.5 mm and evaporation from Lake Taihu was 13.6 mm (Fig. 2). Although some daily mean runoff rates were missing, the change of available daily mean runoff rates (mean: 33.3 ± 1.4 m^3/sec) was stable from December 21 to December 30, 2018 (Fig. 2).

During the *in-situ* observation (from 09:00 LT on December 26 to 12:00 LT on December 29, 2018), the air temperature 10 m above the water surface of Lake Taihu was 0.9 ± 3.4 °C (Fig. 3). The M-K test indicated significant change in the air temperature ($P < 0.01$), from a maximum air temperature of 5.8 °C at 09:00 LT on December 26 to a minimum of −4.9 °C at 07:00 LT on December 29. The wind speed 10 m above the water surface of Lake Taihu was 6.7 ± 1.5 m/sec (Fig. 3). Minimum and maximum wind speeds of 3.0 and 9.1 m/sec were measured at 13:00 LT and 23:00 LT on December 26, respectively. The variation in wind speed was not significant ($P > 0.05$). The wind direction, which was reasonably stable throughout the *in-situ* observation, was dominated by northerly winds (i.e., >315° or <45° for 61.8% of the time). The wind was mainly NE in the early stages of the observation period but became NNW after 12:00 LT on December 28.

2.3. *Variations in water environmental variables*

2.3.1. *Water temperature, pH, DO, and depth*

The mean water temperatures at TH1 and TH2 were 7.59 and 7.60 °C, respectively (Table 3 and Fig. 4). The M-K test suggested the water temperature decreased significantly at both stations, and the water temperatures at TH1 and TH2 were found correlated significantly and positively ($r = 1$, $P < 0.01$). The mean pH values at TH1 and TH2 were 8.29 and 8.15, respectively. The pH increased significantly at TH1 and decreased significantly at TH2. Thus, the water pH values at TH1 and TH2 were correlated significantly and negatively ($r = -0.68$, $P < 0.01$). The DO concentrations averaged 11.85 and 12.17 mg/L at TH1 and TH2, respectively. The DO concentrations increased significantly at both stations. The DO concentrations at TH1 and TH2 were correlated significantly and positively ($r = 0.77$, $P < 0.01$). The mean water depths at TH1 and TH2 were 2.38 and 2.79 m, respectively. There was a significant trend of increase in water depth at both stations. Thus, the water depths at the two stations were correlated significantly and positively ($r = 0.74$, $P < 0.01$).

Table 1 – Mean and standard deviation (SD) of the parameters (median grain size, dry bulk density, water content, and LOI-S) of the sediments at TH1 and TH2, and the significance (P) of the differences of these parameters between TH1 and TH2.

Parameters	Median grain size (μm)		Dry bulk density (kg/m^3)		Water content (%)		LOI-S (g/kg)	
Station	TH1	TH2	TH1	TH2	TH1	TH2	TH1	TH2
Mean ± SD	23.4 ± 1.6	24.1 ± 1.2	899.0 ± 55.2	904.3 ± 47.7	58.2 ± 1.8	57.1 ± 2.2	45.4 ± 1.6	41.4 ± 1.9
P	0.66		0.92		0.61		0.09	

Table 2 – Mean ± standard deviation (SD), background value, and ratio of the mean value to the background value (Ratio) of the contents of nine sediment heavy metals at TH1 and TH2, and the significance (P) of the differences of the contents of nine sediment heavy metals between TH1 and TH2.

Sediment heavy metal	Station	Mean ± SD (mg/kg)	Background (mg/kg)	Ratio	P
Ni	TH1	33 ± 2	16	2.1	0.26
	TH2	32 ± 1		2.0	
Zn	TH1	116 ± 5	59	2.0	0.004
	TH2	96 ± 1		1.6	
As	TH1	13.46 ± 1.43	9.40	1.4	0.065
	TH2	17.33 ± 1.63		1.8	
Mn	TH1	744 ± 64	511	1.5	0.855
	TH2	756 ± 64		1.5	
Cu	TH1	24.8 ± 0.9	18.9	1.3	0.058
	TH2	23.1 ± 0.3		1.2	
V	TH1	87.8 ± 4.6	89.5	1.0	0.37
	TH2	84.2 ± 1.8		0.9	
Co	TH1	13.0 ± 0.7	15.6	0.8	0.191
	TH2	12.2 ± 0.2		0.8	
Mo	TH1	0.63 ± 0.06	\	\	0.004
	TH2	0.36 ± 0.02		\	
Se	TH1	0.40 ± 0.02	\	\	0.017
	TH2	0.34 ± 0.01		\	

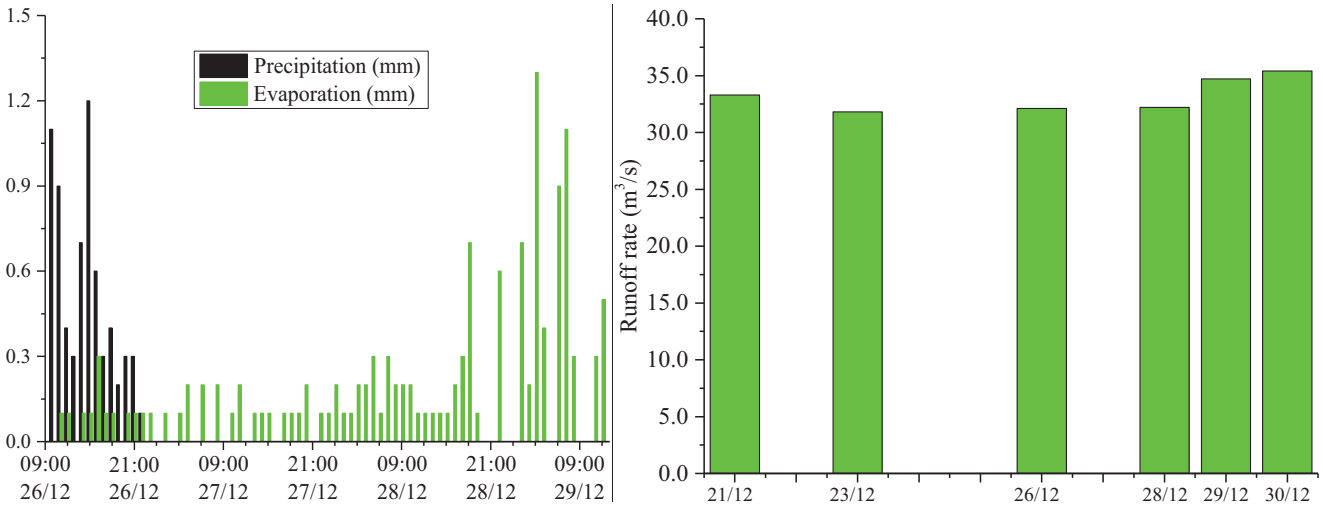

Fig. 2 – Hourly precipitation and evaporation from Dongshan Station and daily mean runoff rate of the Tiaoxi River at Yangjiabu Station in 2018.

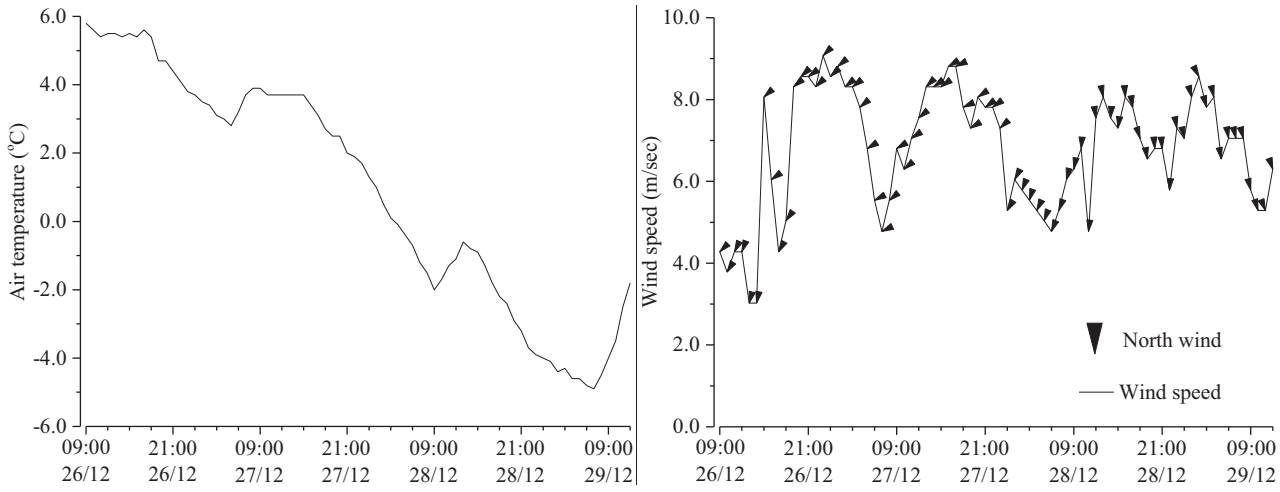

Fig. 3 – Air temperature and wind speed and direction at 10 m above the water surface of Lake Taihu at TH2 in 2018.

Table 3 – Mean ± standard deviation (SD) and *MK* values of the water environmental variables (water temperature, pH, DO, and water depth) at TH1 and TH2, and the Pearson correlation coefficients (*r*) of these variables between TH1 and TH2 between 09:00 LT on December 26 and 12:00 LT on December 29, 2018.

Variable	Temperature (°C)		pH		DO (mg/L)		Water depth (m)	
Station	TH1	TH2	TH1	TH2	TH1	TH2	TH1	TH2
Mean ± SD	7.59 ± 1.32	7.60 ± 1.11	8.29 ± 0.08	8.15 ± 0.09	11.85 ± 0.36	12.17 ± 0.23	2.38 ± 0.08	2.79 ± 0.05
MK	−12.49**	−12.32**	8.60**	−6.68**	12.01**	5.88**	7.32**	5.66**
R	1**		−0.68**		0.77**		0.74**	

*$P < 0.05$,**$P < 0.01$

Table 4 – Mean ± standard deviation (SD) and MK values of the water environmental variables (DOC, LOI-W, Chl*a*, and SS concentrations) at TH1 and TH2, and Pearson correlation coefficients (*r*) of these variables between TH1 and TH2 between 09:00 LT on December 26 and 12:00 LT on December 29, 2018.

Variable	DOC (mg/L)		LOI-W (mg/L)		Chl*a* (μg/L)		SS (mg/L)	
Station	TH1	TH2	TH1	TH2	TH1	TH2	TH1	TH2
Mean ± SD	6.09 ± 0.75	6.73 ± 1.32	26.7 ± 5.1	22.2 ± 4.2	16.65 ± 3.93	27.19 ± 8.57	311.9 ± 93.3	215.1 ± 57.7
MK	−1.93*	−4.19**	2.28*	2.80**	2.90**	−0.82	3.15**	4.89**
R	−0.05		0.66**		0.23		0.82**	

* $P < 0.05$
** $P < 0.01$

2.3.2. *Concentration of DOC, LOI-W, Chl*a*, and ss*

The mean DOC concentrations in the water samples from TH1 and TH2 were 6.09 and 6.73 mg/L, respectively (Table 4 and Fig. 5), and the M-K test showed that the DOC concentrations decreased significantly at both stations. The mean values of LOI-W at TH1 and TH2 were 26.7 and 22.2 mg/L, respectively. The LOI-W concentrations at TH1 and TH2 showed significant increase and were correlated significantly and positively. The mean Chl*a* concentrations within the water column at TH1 and TH2 were 16.65 and 27.19 μg/L, respectively; the concentration at TH1 was increased significantly. Similarly, the mean SS concentrations within the water column at TH1 and TH2 were 311.9 and 215.1 mg/L, respectively. The SS concentrations, which increased markedly at both stations, were correlated significantly and positively.

2.4. *Concentration of dissolved heavy metals*

The average dissolved Ni, Zn, As, Mn, Cu, V, Co, Mo, and Se concentrations at TH1 and TH2 are shown in Table 5 and Fig. 6. There were significant trends of increase in the concentrations of dissolved Ni, Zn, As, Cu, V, Co, Mo, and Se at TH1. Apart from Se, which increased significantly at TH2, the concentrations of dissolved heavy metals mainly decreased at TH2, with significant trends of decrease for Ni, Zn, As, Cu, and V. The concentrations of dissolved As or V at TH1 were significantly and negatively correlated to the concentrations of dissolved As or V at TH2, while the concentrations of dissolved Se at TH1 were significantly and positively correlated to the concentrations of dissolved Se at TH2.

The significant correlations between these dissolved heavy metals at TH1 or TH2 were positive (Table 6). Dissolved

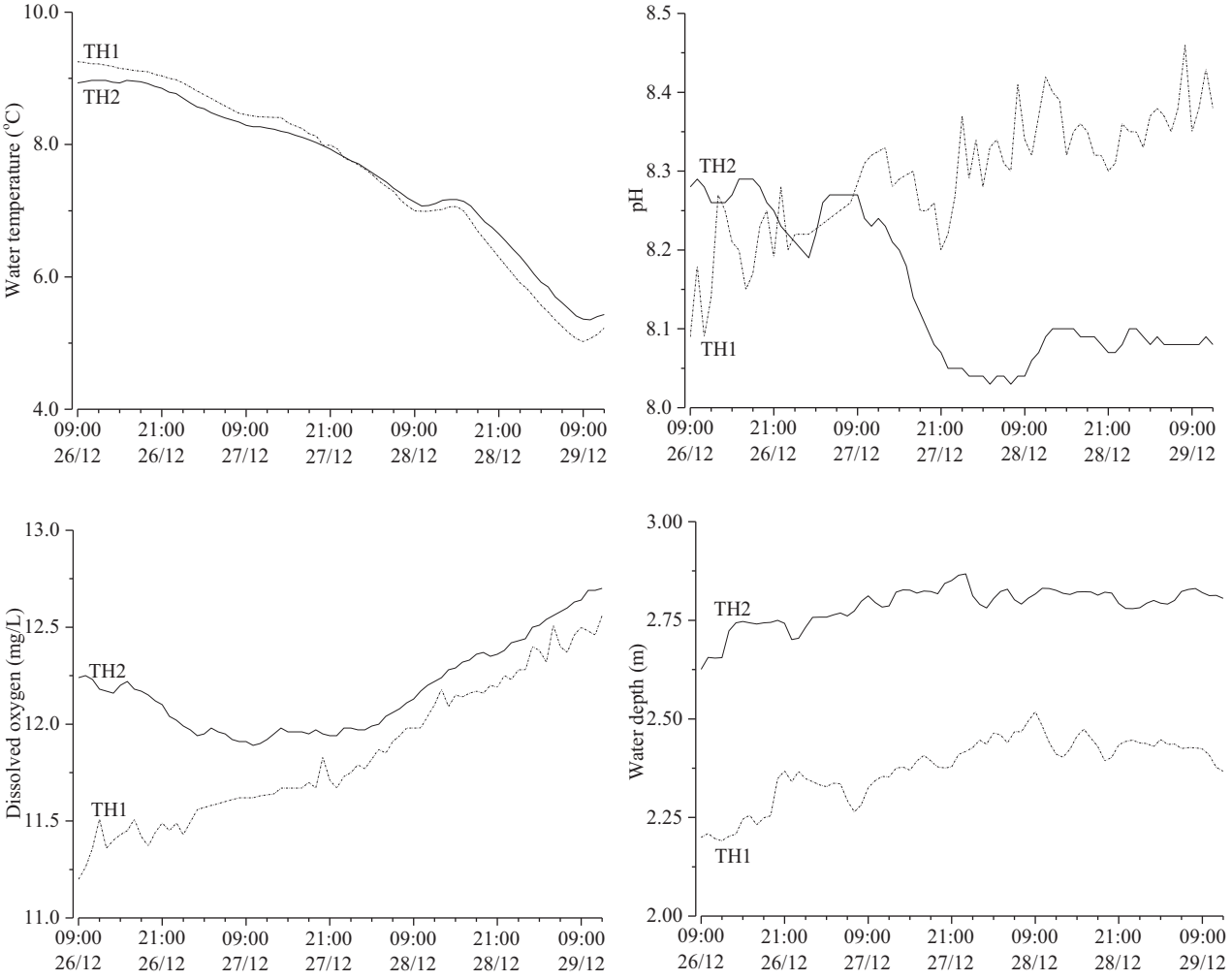

Fig. 4 – Variations in water temperature, pH, DO, and water depth in the overlying water at TH1 and TH2 in 2018.

Zn had no significant correlation with the other dissolved heavy metals at TH1. Excluding dissolved Zn, dissolved V was correlated significantly with the other heavy metals at TH1. Dissolved Mo or Se had no significant correlation with the other dissolved heavy metals at TH2. Excluding dissolved Mo and Se, dissolved Ni was correlated significantly with the other heavy metals at TH2.

3. Discussion

The sediment investigation indicated no significant differences between the physical characteristics of the sediments at TH1 (estuary area) and TH2 (lake center). The contents of most heavy metals in the sediments were also similar. The *in-situ* observations indicated that Lake Taihu experienced strong northerly winds between 09:00 LT on December 26 and 12:00 LT on December 29, and the sediment concentrations in the overlying water at both lake areas increased significantly. The water environmental variables also varied considerably. With the exception of Mo and Se, the concentrations of the dissolved heavy metals tended to decrease in the lake center, but increased in the estuary area. The results suggested that the trends for the release of internal dissolved heavy metals in different areas of the same lake were completely different.

3.1. *Characteristics of heavy metals in the sediments*

The contents of Ni, Zn, As, Mn, and Cu in the sediments in Lake Taihu were 1.2–2.1 times the corresponding background values in the soils of the Lake Taihu Basin (Tao et al., 2012), and the sediments were continually being enriched with heavy metals in the lake. The contents of V and Co in the sediments were close to the corresponding background values (Table 2). These results are consistent with those of previous researchers (Liu et al., 2012; Qu et al., 2001; Tao et al., 2012). Their findings suggested that enrichment of Ni, Zn, As, Mn, and Cu in sediments was related primarily to external inputs associated with anthropogenic activities via river discharge, atmospheric deposition, and shipping. The contents of sediment Zn, Mo, and Se were significantly higher in the estuary area than in the lake center ($P < 0.05$), which also confirms that exogenous heavy metal inputs contribute to the enrichment of heavy metals in the sediments of Lake Taihu. However, the contents of sediment V and Co mainly reflected natural processes such as weathering and erosion of the parent rock or soil. This is one of main causes of the significant correlation between dissolved V concentration and dissolved Co concen-

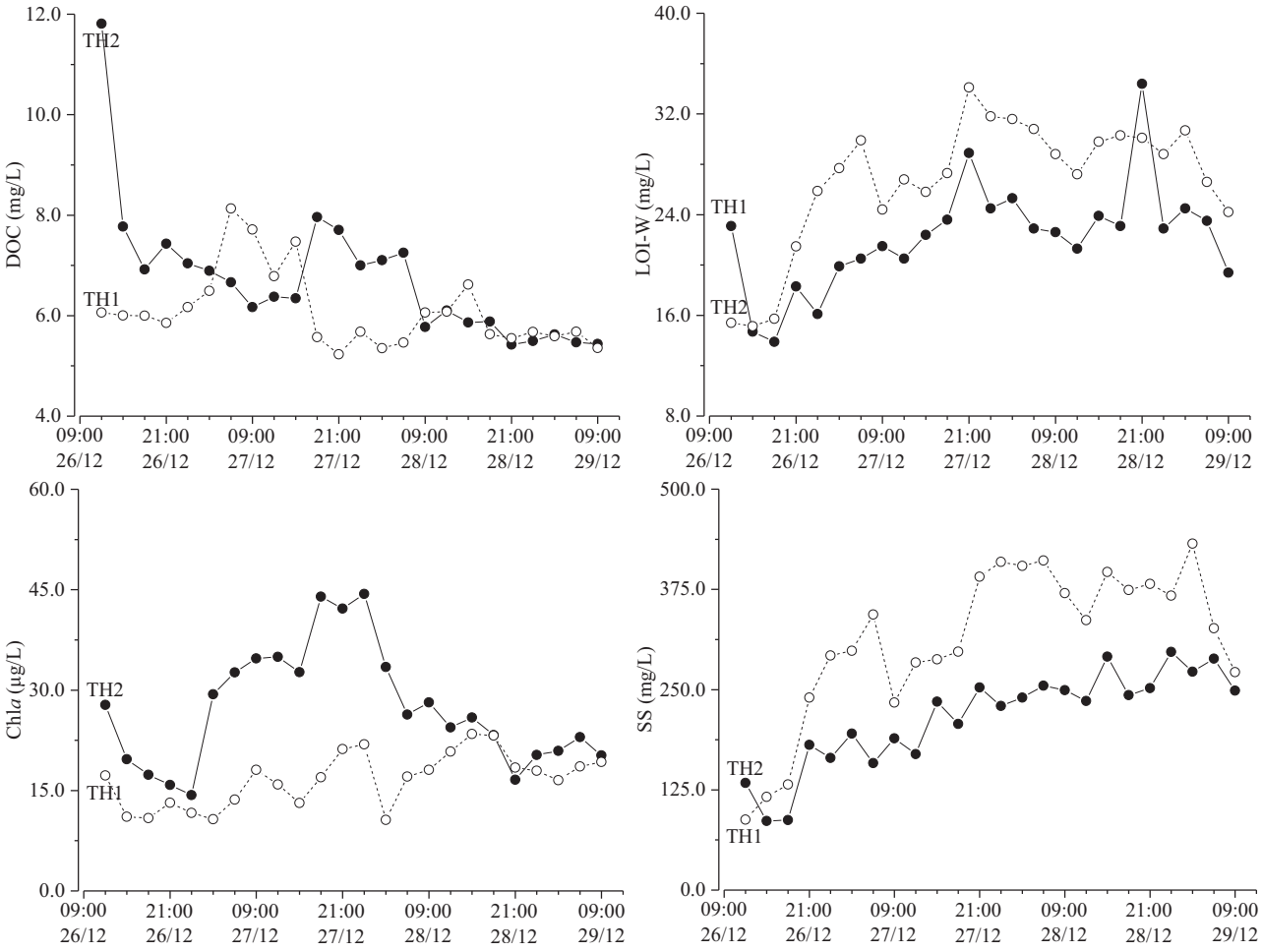

Fig. 5 – Variations in DOC, LOI-W, Chl*a*, and SS concentrations in the overlying water at TH1 and TH2 in 2018.

tration in the overlying water at TH1 or TH2 during the *in-situ* observations (Table 6).

The physical and chemical characteristics of the sediments in Lake Taihu determine the release of heavy metals from the surface sediments into the overlying water. The sediment investigation indicated that the surface sediments have water content of 57.6%, median grain size of 23.7 μm, and dry bulk density of 901.6 kg/m^3, which means they can be defined as cohesive sediments. Such sediments have weak shear resistance (0.03–0.04 N/m^2) (Qin et al., 2004), which means they are susceptible to erosion and resuspension under even slight hydrodynamic disturbance (Wu et al., 2016). When sediments are resuspended, heavy metals in the sediments are synchronously transported into the overlying water (Guo et al., 2018).

3.2. In-situ *resuspension of particulate heavy metals*

During our *in-situ* observation in the dry season of Lake Taihu, the amount of precipitation was insufficient to exceed evaporation (Fig. 2), and it did not change significantly the runoff rate and sediment transport rate of the Tiaoxi River. The daily mean runoff rates of the Tiaoxi River changed little before and during the northerly winds (Fig. 2). Moreover, under these stable runoff rates, the SS concentration in the overlying water at 12:00 LT on December 26 at TH1 (88 mg/L) was less than at TH2 (133.5 mg/L). The distance between TH1 and the mouth of the Tiaoxi River (3.8 km) is shorter than that between TH2 and the mouth of the Tiaoxi River (15.9 km). Therefore, the Tiaoxi River did not contribute to the continuous increase of SS concentration in the overlying water at either TH1 or TH2 during the *in-situ* observation (Fig. 5).

The increase of SS in the overlying water resulted from sediment resuspension. Qin et al. (2004) and Wu et al. (2016) proved that wind-induced waves could cause sediment resuspension and increase the SS concentration in overlying water. They found that sediment would be resuspended when the wind speed was >4 m/*sec*. Moreover, when the disturbance intensity was constant, the SS concentration in the overlying water would increase with the duration of the disturbance. Apart from the first 6 hr, the wind speed over Lake Taihu was > 4 m/sec throughout the observation period (Fig. 3), and the SS concentration in the overlying water increased continually (Fig. 5 SS) at both stations. However, the SS concentration at TH1 was significantly higher than that at TH2 (Fig. 5 SS) because of the dissipation of wind wave energy. The water depth at TH1 (2.37 ± 0.08 m) was significantly lower than at TH2 (2.78 ± 0.06 m). When the wind waves propagated from TH2 to TH1, wave energy was dissipated because of bottom friction and depth-induced wave breaking, which can increase the disturbance at the water–sediment interface and cause sediment resuspension.

The resuspension of sediments rich in pollutants inevitably leads to overall increase in pollutant concentrations in the overlying water. During the northerly wind event, the LOI-W concentration was found correlated significantly with

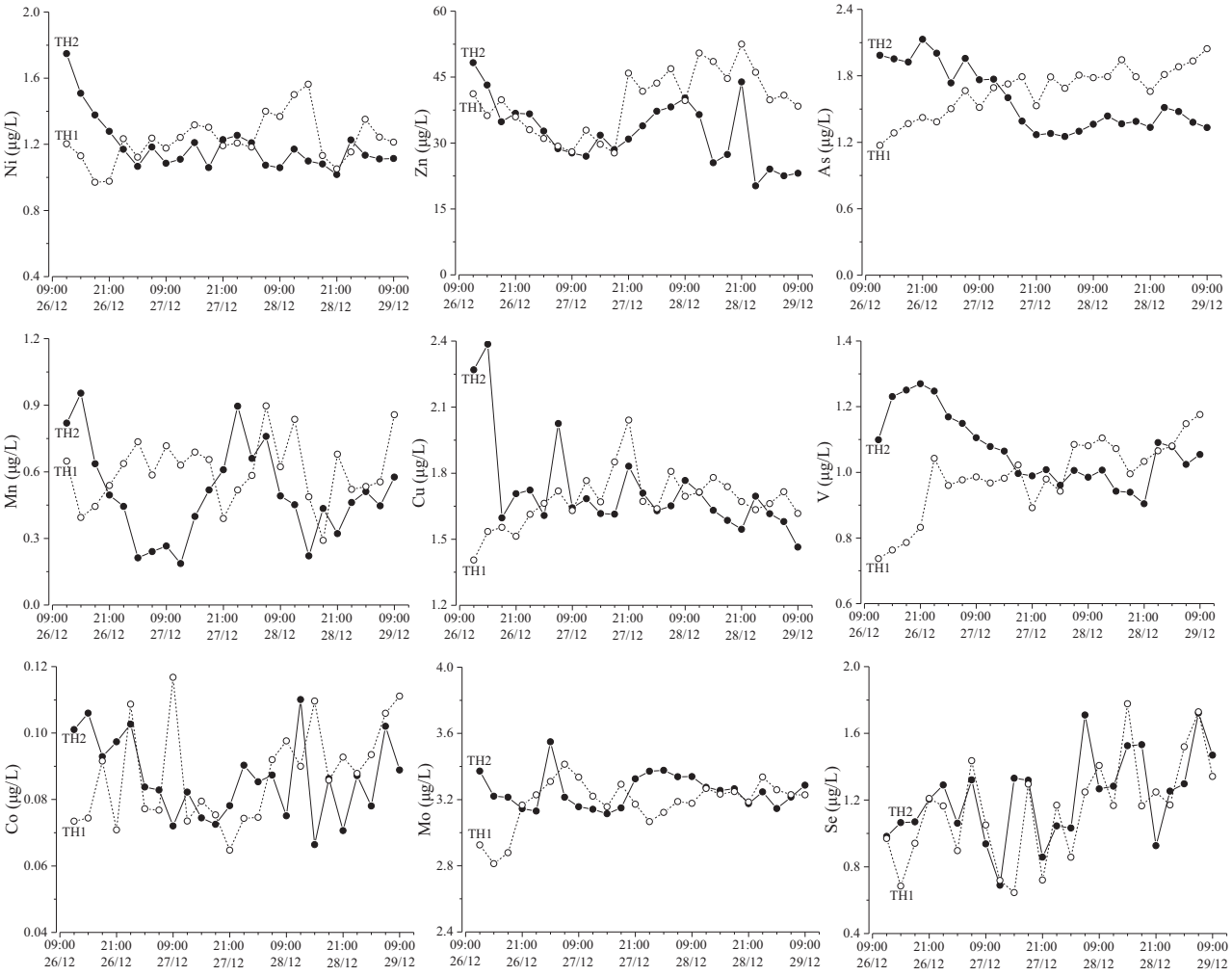

Fig. 6 – Variations of the dissolved heavy metal concentrations in the overlying water at TH1 and TH2 in 2018.

SS ($P < 0.01$) at both stations. When the sediments were resuspended, particulate organic matter was released, causing the LOI-W concentration in the overlying water at TH1 and TH2 to increase by as much 1.25 and 1.47 times, respectively (Fig. 5 LOI-W). Similarly, the heavy metals enriched in the sediments can also be resuspended (Dong et al., 2019; Eggleton and Thomas, 2004; Jonge et al., 2012). Using the sediment Zn content as an example (Table 2), we calculated that resuspension of the sediments caused the Zn concentration to increase by as much as 39.98 and 20.18 μg/L at TH1 and TH2, respectively.

3.3. In-situ *release of dissolved heavy metals*

During the northerly wind event, the concentrations of dissolved Ni, Zn, As, Cu, V, Co, Mo, and Se in the overlying water at TH1 increased significantly (Table 5 and Fig. 6). The SS concentration was correlated positively and significantly with the concentration of dissolved Ni, As, Cu, V, Mo, and Se at TH1 (Table 7). These results show that sediment suspension caused the release of dissolved heavy metal at TH1. However, apart from dissolved Mo, and Se, the changes of other dissolved heavy metal concentrations with time at TH2 were opposite those at TH1 during the northerly wind event (Table 5 and Fig. 6). The concentrations of dissolved Ni, Zn, As, Cu, and V in the overlying water at TH2 decreased significantly (Table 5 and Fig. 6). The SS concentration was correlated negatively and significantly with the concentrations of dissolved Ni, Zn, As, Cu, and V at TH2 (Table 8). These results show that sediment resuspension caused the decrease of the concentrations of most dissolved heavy metals at TH2.

Sediment resuspension caused release of dissolved Se and Mo. The concentration of dissolved Se increased significantly ($P < 0.05$) at both stations during the northerly wind event. The dissolved Se concentration in the water column was significantly correlated with the DO, water temperature, and SS concentration ($P < 0.05$). Therefore, the northerly wind caused the release of dissolved Se from the sediments into the water column. Similar to the dissolved Se concentration, the dissolved Mo concentration increased ($P < 0.01$, TH1) or decreased ($P > 0.05$, TH2) with the increase of dissolved V concentration at TH1 (Table 6), but its trend was not significant at TH2 ($P > 0.05$, Table 5).

Apart from Mo and Se, the concentrations of the other dissolved heavy metals showed opposite patterns between the two stations, i.e., increase at TH1 and decrease at TH2 during the northerly wind event (Table 5). Although the trend of change of dissolved Mn concentration at both stations and dissolved Co concentration at TH2 were not significant, the dissolved Mn or Co concentration was correlated significantly and positively with dissolved V concentration (Table 6). As confirmed in previous studies, the concentrations of dissolved heavy metals are determined by the adsorption equilib-

Table 5 – Mean ± standard deviation (SD) and *MK* values of dissolved heavy metal concentrations at TH1 and TH2, and Pearson correlation coefficients (*r*) of the concentrations between TH1 and TH2 between 09:00 LT on December 26 and 12:00 LT on December 29, 2018.

Dissolved heavy metal	Station	Mean ± SD (μg/L)	*MK*	*r*
Ni	TH1	1.23 ± 0.14	1.76*	−0.292
	TH2	1.19 ± 0.16	−2.36**	
Zn	TH1	39.33 ± 7.12	1.81*	0.166
	TH2	32.49 ± 7.18	−2.51**	
As	TH1	1.67 ± 0.22	5.18**	−0.759**
	TH2	1.58 ± 0.28	−3.20**	
Mn	TH1	0.6 ± 0.15	0.20	−0.157
	TH2	0.5 ± 0.21	−0.45	
Cu	TH1	1.68 ± 0.12	1.91*	−0.324
	TH2	1.72 ± 0.21	−2.65**	
V	TH1	0.99 ± 0.11	4.42**	−0.506**
	TH2	1.07 ± 0.1	−3.45**	
Co	TH1	0.09 ± 0.01	2.31*	−0.134
	TH2	0.09 ± 0.01	−0.64	
Mo	TH1	3.19 ± 0.14	1.69*	−0.102
	TH2	3.25 ± 0.01	0.07	
Se	TH1	1.15 ± 0.3	2.70**	0.673**
	TH2	1.22 ± 0.26	2.08*	

* $P < 0.05$
** $P < 0.01$

rium, which is related to the environmental variables, e.g., water temperature, pH, DO, and SS concentration (Eggleton and Thomas, 2004; Linge and Oldham, 2002; Xu et al., 2017). The T Test showed that the environmental variable (i.e., pH, DO, water depth, LOI-W, Chl*a*, or SS) was significantly different between TH1 and TH2 ($P < 0.01$), whereas temperature and DOC exhibited no significant difference between the two stations ($P > 0.05$; Figs. 4 and 5). Moreover, apart from pH and Chl*a* concentration, the correlation analysis indicated that DO, water depth, LOI-W, or SS concentration at TH1 was correlated significantly and positively with that at TH2 (Tables 3 and 4). Apart from pH and Cha concentration, the changing trend of DO, water depth, LOI-W, or SS concentration at TH1 was similar to that at TH2. Therefore, the contrasting trends of the dissolved heavy metal concentrations at the two stations cannot be explained by the changes of temperature, DO, water depth, DOC, LOI-W, or SS concentration; instead, they were more likely related to pH or Chl*a* concentration.

Table 7 – Correlation coefficients (*r*) and significance (*P*) between the dissolved heavy metal concentrations and water environmental variables at TH1 between 09:00 LT on December 26 and 12:00 LT on December 29, 2018.

Dissolved Heavy metal	Water temperature	pH	DO	DOC	LOI-W	Chl*a*	SS
Ni	−0.3	0.53**	0.36	0.13	0.39	0.43*	0.44*
Zn	−0.5*	0.36	0.54**	−0.59**	0.29	0.53**	0.4
As	−0.83**	0.85**	0.83**	−0.17	0.64**	0.55**	0.72**
Mn	−0.12	0.22	0.12	0.14	0.04	−0.08	0.03
Cu	−0.24	0.29	0.23	−0.12	0.74**	0.45*	0.64**
V	−0.79**	0.81**	0.78**	−0.1	0.62**	0.45*	0.68**
Co	−0.47*	0.38	0.47*	0.1	0.01	0.25	0.1
Mo	−0.38	0.46*	0.4	0.26	0.66**	0.27	0.6**
Se	−0.59**	0.43*	0.62**	−0.09	0.29	0.45*	0.42*

* $P < 0.05$
** $P < 0.01$

Table 6 – Correlation coefficients (*r*) and significance (*P*) between the dissolved heavy metal concentrations at TH1 (blue cells) or at TH2 (yellow cells) between 09:00 LT on December 26 and 12:00 LT on December 29, 2018.

Dissolved heavy metal	Ni	Zn	As	Mn	Cu	V	Co	Mo	Se
Ni		0.49*	0.53**	0.63**	0.77**	0.45*	0.54**	0.11	−0.31
Zn	0.18		0.27	0.46*	0.52**	0.12	0.30	0.24	−0.34
As	0.55**	0.26		−0.07	0.50*	0.89**	0.40	−0.29	−0.29
Mn	0.34	−0.11	0.21		0.46*	0.09	0.48*	0.26	−0.00
Cu	0.41*	0.15	0.48*	−0.06		0.36	0.41*	0.11	−0.28
V	0.57**	0.19	0.87**	0.44*	0.41*		0.48*	−0.20	−0.18
Co	0.30	0.09	0.37	0.30	−0.09	0.61**		0.10	0.10
Mo	0.32	−0.16	0.55**	0.31	0.45*	0.69**	0.28		−0.05
Se	0.41*	0.24	0.59**	0.08	0.10	0.63**	0.58**	0.43*	

*$P < 0.05$.
**$P < 0.01$.

Table 8 – Correlation coefficients (r) and significance (P) between the dissolved heavy metal concentrations and water environmental variables at TH2 between 09:00 LT on December 26 and 12:00 LT on December 29, 2018.

Dissolved heavy metal	Water temperature	pH	DO	DOC	LOI-W	Chl*a*	SS
Ni	0.5**	0.48*	−0.04	0.78**	−0.33	−0.1	−0.6**
Zn	0.53**	0.17	−0.31	0.59**	0.01	−0.13	−0.49*
As	0.71**	0.93**	−0.28	0.42*	−0.68**	−0.34	−0.81**
Mn	0.12	−0.15	0.07	0.51*	−0.13	0.03	−0.25
Cu	0.52**	0.45*	−0.21	0.67**	−0.26	0.04	−0.58**
V	0.59**	0.8**	−0.19	0.27	−0.81**	−0.38	−0.73**
Co	0.16	0.23	0.18	0.32	−0.53**	−0.41*	−0.40
Mo	0	−0.28	−0.08	0.26	0.12	0.24	0.1
Se	−0.51*	−0.38	0.48*	−0.31	−0.1	−0.29	0.46*

* $P < 0.05$
** $P < 0.01$

During the northerly wind event, the pH at TH1 was correlated significantly negatively with the pH at TH2 (Table 3). Moreover, pH was correlated positively with the concentrations of dissolved Ni, Zn, As, Cu, V, and Co at both stations, of which the correlations between pH and dissolved Ni, As, and V were significant at both stations (Tables 7 and 8). For example, the correlation coefficients between pH and dissolved As concentration reached 0.85 and 0.93 ($P < 0.01$) at TH1 and TH2, respectively, and the trend of change of pH at TH1 or TH2 was similar to that of dissolved As concentration. Previous laboratory simulations found that pH is a determining factor of the adsorption equilibrium between heavy metals and SS within the water column (Linge and Oldham, 2002; Mamat et al., 2016; Peng et al., 2009). Therefore, it can be inferred that the differences in the trend of change of pH between the two stations resulted in the contrasting trends of dissolved heavy metal concentrations at two stations by influencing the adsorption equilibrium of heavy metals between the water column and the SS.

The Chl*a* concentration difference between the two studied is another major reason for the contrasting trends during the northerly wind event. It has been confirmed that phytoplankton dominated by cyanobacteria not only proliferate rapidly in Lake Taihu in summer and autumn, but also can maintain their cell viability and form blooms during winter (Ma et al., 2016). The formation of such blooms means that the distribution of cyanobacteria has marked temporal and spatial differences (Wu et al., 2019), which resulted in the average Chl*a* concentration at TH2 being 2.12 times that at TH1 during the Chl*a* concentration peak at TH2 between 06:00 LT on December 27 and 09:00 LT on December 28 (Fig. 5). The abnormally high biomass of cyanobacteria in the overlying water at TH2 directly caused the concentrations of dissolved heavy metals to decrease through growth-related assimilation or surface adsorption of cyanobacteria (Baptista et al., 2014; Jia et al., 2018; Peel et al., 2009).

Moreover, cyanobacteria can also indirectly affect dissolved heavy metal concentrations by influencing the water pH and DO (O'Neil et al., 2012; Paerl and Paul, 2012; Pokrovsky and Shirokova, 2013). Zhang et al. (2015) found that pH variation in Lake Taihu is determined by phytoplankton growth. During the northerly wind event, the inflections of pH at TH2, which coincided with the Chl*a* concentration peak (Fig. 4), were caused by the limiting factors of low water temperature (Table 3) and light induced by the high SS concentration (Table 4) during the *in-situ* observations. Therefore, phytoplankton growth was inhibited and it was considered to have caused little change to the pH of the overlying water. Moreover, the DO curve also exhibited similar response during the peak.

4. Conclusions

In Lake Taihu, *in-situ* observation indicated that the strong northerly winds caused sediment and particulate heavy metal resuspension. However, the concentrations of most dissolved heavy metals showed opposite patterns between the two lake areas studied, i.e., they increased in the estuary area but decreased in the lake center. This contrasting trend resulted primarily from the fluctuation of pH and Chl*a* concentration related to lake eutrophication. The other environmental variables might have affected the release of dissolved heavy metals, but further research will be required to verify this speculation. It can also be inferred that consideration of the appropriate sampling frequency, location, and environmental variables is very important for reliable monitoring and risk assessment of heavy metals in shallow eutrophic lakes.

Acknowledgments

This work was supported by the National Key R&D Program of China (No. 2017YFC0405205), the National Natural Science Foundation of China (Nos. 41971047, 41621002, 41661134036, 41301531), the Key Research Program of Frontier Sciences, Chinese Academy of Sciences (No. QYZDJ-SSW-DQC008), and the "One-Three-Five" Strategic Planning of the Nanjing Institute of Geography and Limnology, Chinese Academy of Sciences (No. NIGLAS2017GH04). The authors thank Dr. Yin Hongbin of the Nanjing Institute of Geography and Limnology, Chinese Academy of Sciences, for scientific suggestions.

Appendix A. Supplementary

Supplementary material associated with this article can be found, in the online version, at doi:10.1016/j.jes.2020.05.004.

REFERENCES

American Public Health Association (APHA), 1998. Standard Methods for the Examination of Water and Wastewater, 20th ed American Public Health Association, Washington, DC.

Baptista, M.S., Vasconcelos, V.M., Vasconcelos, M.T.S.D., 2014. Trace metal concentration in a temperate freshwater reservoir seasonally subjected to blooms of toxin-producing cyanobacteria. Microb. Ecol. 68 (4), 671–678.

Beutel, M.W., Leonard, T.M., Dent, S.R., Moor, B.C., 2008. Effects of aerobic and anaerobic conditions on P, N, Fe, Mn and Hg accumulation in waters overlaying profundal sediments of an oligo-mesotrophic lake. Water Res. 42, 1953–1962.

Boyle, J., 2004. A comparison of two methods for estimating the organic matter content of sediments. J. Paleolimnol. 31, 125–127.

Chen, Y.W., Gao, X.Y., 2000. Comparison of two methods for phytoplankton chlorophyll-a concentration measurement. J. Lake Sci. 12, 185–188 (In Chinese with English abstract).

Cózar, A., Gálvez, J.A., Hull, V., García, C.M., Loiselle, S.A., 2005. Sediment resuspension by wind in a shallow lake of *Esteros del Iberá* (Argentina): a model based on turbidimetry. Ecol. Model 186, 63–76.

Ding, Y., Qin, B., Zhu, G., Wu, T., Wang, Y., Luo, L., 2012. Effects of typhoon Morakot on a large shallow lake ecosystem, Lake Taihu, China. Ecohydrology 5, 798–807.

Dong, J., Xia, X., Liu, Z., Zhang, X., Chen, Q., 2019. Variations in concentrations and bioavailability of heavy metals in rivers during sediment suspension-deposition event induced by dams: insights from sediment regulation of the Xiaolangdi Reservoir in the Yellow River. J. Soil Sediment 19, 403–414.

Eggleton, J., Thomas, K.V., 2004. A review of factors affecting the release and bioavailability of contaminants during sediment disturbance events. Environ. Int. 30 (7), 973–980.
Geng, D., Yang, F., Wei, C., Ji, H., 2015. Effects of wind-wave disturbance on the partition of arsenic between the water-suspended solids phase of Lake Taihu. Acta Scientiae Circumstantiae 35 (5), 1358–1365.
Graca, B., Burska, D., Matuszewska, K., 2004. The impact of dredging deep pits on organic matter decomposition in sediments. Water Air Soil Poll 158, 237–259.
Guo, B., Liu, Y., Zhang, F., Hou, J., Zhang, H., Li, C., 2018. Heavy metals in the surface sediments of lakes on the Tibetan Plateau, China. Environ Sci Pollut Res 25, 3695–3707.
Hofmann, H., Lorke, A., Peeters, F., 2008. The relative importance of wind and ship waves in the littoral zone of a large lake. Limnol. Oceanogr. 53, 368–380.
Hou, D., O'Connor, D., Nathanail, P., Tian, L., Ma, Y., 2017. Integrated GIS and multivariate statistical analysis for regional scale assessment of heavy metal soil contamination: A critical review. Environ. Pollut. 231, 1188–1200.
Jiang, X., Wang, W., Wang, S., Zhang, B., Hu, J., 2012. Initial identification of heavy metals contamination in Taihu Lake, a eutrophic lake in China. J. Environ. Sci. 24 (9), 1539–1548.
Jia, Y., Chen, W., Zuo, Y., Lin, L., Song, L., 2018. Heavy metal migration and risk transference associated with cyanobacterial blooms in eutrophic freshwater. Sci. Total Environ. 613–614, 1324–1330.
Jin, K.R., Ji, Z.G., 2001. Calibration and verification of a spectral wind-wave model for Lake Okeechobee. Ocean. Eng. 28, 571–584.
Jonge, M.D., Teuchies, J., Meire, P., Blust, R., Bervoets, L., 2012. The impact of increased oxygen conditions on metal-contaminated sediments part I: Effects on redox status, sediment geochemistry and metal bioavailability. Water Res 46, 2205–2214.
Li, Y., Zhou, S., Zhu, Q., Li, B., Wang, J., Wang, C., et al., 2018. One-century sedimentary record of heavy metal pollution in western Taihu Lake, China. Environ. Pollut. 240, 709–716.
Linge, K.L., Oldham, C.E., 2002. Arsenic remobilization in a shallow lake: the role of sediment resuspension. J. Environ. Qual. 31 (3), 822.
Liu, E., Birch, G.F., Shen, J., Yuan, H., Zhang, E., Cao, Y., 2012. Comprehensive evaluation of heavy metal contamination in surface and core sediments of Taihu Lake, the third largest freshwater lake in China. Environ. Earth. Sci. 67 (1), 39–51.
Liu, J., Wang, P., Wang, C., Qian, J., Hou, J., 2017. Heavy metal pollution status and ecological risks of sediments under the influence of water transfers in Taihu Lake, China. Environ. Sci. Pollut. Res. 24, 2653–2666.
Ma, J., Qin, B., Paerl, H.W., Brookes, J.D., Hall, N.S., Shi, K., et al., 2016. The persistence of cyanobacterial (*Microcystis* spp.) blooms throughout winter in Lake Taihu, China. Limnol. Oceanogr. 61 (2), 711–722.
Mamat, Z., Haximu, S., Zhang, Z., Aji, R., 2016. An ecological risk assessment of heavy metal contamination in the surface sediments of Bosten Lake, northwest China. Environ Sci Pollut Res 23, 7255–7265.
Niu, Y., Jiao, W., Yu, H., Yu, Niu, Y., Pang, Y., Xu, X., et al., 2015. Spatial evaluation of heavy metals concentrations in the surface sediment of Taihu Lake. Int. J. Env. Res. Pub. He. 12, 15028–15039.
O'Neil, J.M., Davis, T.W., Burford, M.A., Gobler, C.J., 2012. The rise of harmful cyanobacteria blooms: The potential roles of eutrophication and climate change. Harmful Algae 14, 313–334.
Paerl, H.W., Paul, V.J., 2012. Climate change: links to global expansion of harmful cyanobacteria. Water Res 46 (5), 1349–1363.
Peel, K., Weiss, D., Sigg, L., 2009. Zinc isotope composition of settling particles as a proxy for biogeochemical processes in lakes: insights from the eutrophic Lake Greifen, Switzerland. Limnol. Oceanogr 54 (5), 1699–1708.
Peng, J., Song, Y., Yuan, P., Cui, X., Qiu, G., 2009. The remediation of heavy metals contaminated sediment. J. Hazard. Mater. 161, 633–640.
Pokrovsky, O.S., Shirokova, L.S., 2013. Diurnal variations of dissolved and colloidal organic carbon and trace metals in a boreal lake during summer bloom. Water Res 47 (2), 922–932.
Porter, J., Arzberger, P., Braun, H.W., Bryant, P., Gage, S., Hansen, T., et al., 2005. Wireless sensor networks for ecology. Bioscience 55, 561–572.
Qin, B.Q., Hu, W.P., Gao, G., Luo, L.C., Zhang, J., 2004. Dynamics of sediment resuspension and the conceptual schema of nutrient release in the large shallow Lake Taihu, China. Chin. Sci. Bull. 49, 54–64.
Qin, B., Xu, P., Wu, Q., Luo, L., Zhang, Y., 2007. Environmental issues of Lake Taihu, China. Hydrobiologia 581, 1–3.
Qu, W., Dickman, M., Wang, S., 2001. Multivariate analysis of heavy metal and nutrient concentrations in sediments of Taihu Lake, China. Hydrobiologia 450 (1–3), 83–89.
Ramaswamy, V., Rao, P.S., 2006. Grain size analysis of sediments from the northern Andaman Sea: comparison of laser diffraction and sieve-pipette techniques. J. Coastal Res. 22 (4), 1000–1009.
Shen, J., Yuan, H., Liu, E., Wang, J., Wang, Y., 2011. Spatial distribution and stratigraphic characteristics of surface sediments in Taihu Lake, China. Chin. Sci. Bull. 56, 179–187.
Tang, C., Li, Y., He, C., Acharya, K., 2020. Dynamic behavior of sediment resuspension and nutrients release in the shallow and wind-exposed Meiliang Bay of Lake Taihu. Sci. Total Environ. 708, 135131.
Tao, Y., Zhang, Y., Meng, W., Hu, X., 2012. Characterization of heavy metals in water and sediments in Taihu Lake, China. Environ. Monit. Assess 184 (7), 4367–4382.
Wang, Q., Zhang, Y., Wang, X., Wang, Y., Meng, G., Chen, Y., 2020. The adsorption behavior of metals in aqueous solution by microplastics effected by UV radiation. J. Environ. Sci. 87, 272–280.
Wu, T., Qin, B., Brookes, J.D., Yan, W., Ji, X., Feng, J., 2019. Spatial distribution of sediment nitrogen and phosphorus in Lake Taihu from a hydrodynamics-induced transport perspective. Sci. Total Environ. 650, 1554–1565.
Wu, T., Qin, B., Ding, W., Zhu, G., Zhang, Y., Gao, G., et al., 2018. Field observation of different wind-induced basin-scale current field dynamics in a large, polymictic, eutrophic lake. J. Geophys. Res-Oceans 123, 6945–6961.
Wu, T., Timo, H., Qin, B., Zhu, G., Janne, R., Yan, W., 2016. *In-situ* erosion of cohesive sediment in a large shallow lake experiencing long-term decline in wind speed. J. Hydrol. 539, 254–264.
Xu, Y., Wu, Y., Han, J., Li, P., 2017. The current status of heavy metal in lake sediments from china: pollution and ecological risk assessment. Ecol. Evol. 7, 5454–5466.
Yin, H., Cai, Y., Duan, H., Gao, J., Fan, C., 2014. Use of DGT and conventional methods to predict sediment metal bioavailability to a field inhabitant freshwater snail (*Bellamya aeruginosa*) from Chinese eutrophic lakes. J. Hazard. Mater 264, 184–194.
Zhang, X., Zhou, X., Li, Q., Jiang, F., 2015. Seasonal variation regularity and mutation cause of pH in raw water of Taihu Lake. Water Technology 9 (5), 13–17.
Zhu, G, Chi, Q., Qin, B., Wang, W., 2005a. Heavy-metal contents in suspended solids of Meiliang Bay, Taihu Lake and its environmental significances. J. Environ. Sci. 17 (4), 672–675.
Zhu, G, Qin, B., Gao, G., 2005b. Direct evidence of phosphorus outbreak release from sediment to overlying water in a large shallow lake caused by strong wind wave disturbance. Chin. Sci. Bull. 50 (6), 577–582.